EXAFS studies of a chiral rhenium lactone complex and its precursors including multiple scattering calculations*

Teja S. Ertel**, Sabine Hückmann and Helmut Bertagnolli
Institut für Physikalische Chemie, Universität Stuttgart, Pfaffenwaldring 55, D-70569 Stuttgart (Germany)

Gerhard Bringmann and Olaf Schupp
Institut für Organische Chemie, Universität Würzburg, Am Hubland, D-97074 Würzburg (Germany)

(Received December 31, 1993)

Abstract

EXAFS studies of a chiral rhenium complex with an 'axially prostereogenic' biaryl lactone as ligand and its precursors in CH_2Cl_2 and acetone solutions, respectively, are presented. The results of the data analysis for the precursors $CpRe(CO)_3$, $[CpRe(CO)_2(NO)]BF_4$ and $[CpRe(CO)(NO)(PPh_3)]BF_4$ in acetone, obtained with the commonly used single-electron single-scattering theory with different theoretical amplitude and phase functions, are compared with those obtained by including multiple scattering effects. It is shown that the EXAFS spectroscopical investigation of a series of compounds with known structures and with an increasing degree of complexity is a great help for interpreting the EXAFS function of a related compound for which the structure in solution is unknown.

Key words: EXAFS; Molecular structure; Rhenium complexes; Chiral complexes

1. Introduction

Chiral rhenium complexes of the general type $CpRe^*(NO)(PPh_3)L$ (*: stereogenic center) have been found to be very useful substrates for the stereoselective reduction and alkylation of aldehydes and ketones [2]. Starting from the known precursors **1–3** [3], some of us (G.B. and O.S.) [4] recently synthesized related rhenium complexes of type **4**, with 'axially prostereogenic' biaryl lactones (denoted by L) as ligands, aiming at the stereocontrolled ring cleavage of these interesting species for the atropoenantioselective construction of sterically hindered and thus chiral biaryl systems [5]. For a better understanding of the mechanism [6, 7] of this interesting process or even a prediction of the stereochemical outcome of the nucleophilic attack to the activated carbonyl group, a better knowledge of the structures of the active species, not only in the crystalline solid state but also in homogeneous solution, would be highly desirable. For this reason we performed EXAFS investigations with complexes **1–4** (see Fig. 1) in acetone or CH_2Cl_2 solution and compared the results with those obtained by X-ray structure analysis of the crystalline compounds and their analogues.

Extended X-ray absorption fine structure (EXAFS) is based upon the absorption of X-rays by a particular absorbing atom and the oscillatory variation of the X-ray absorption coefficient μ as a function of the photon energy E beyond an absorption edge. The modulation of $\mu(E)$ provides information about the kind, number and distance of neighbors surrounding the absorbing atom. The EXAFS phenomenon is independent of the state of matter and therefore suitable for the determination of structural parameters in solution [8, 9].

2. Experimental

The EXAFS experiment was carried out at the Re-L_{III}-edge at 10 531.0 eV at the beam line RÖMO II at the Hamburger Synchrotronstrahlungslabor (HASYLAB) at DESY, Hamburg, at 20 °C with a Si(311) crystal monochromator under ambient conditions (5.4 GeV, beam current 40 mA). A sample cell suitable for measuring air- and moisture-sensitive liquid compounds, adjustable with high precision between 35.000 and 0.0

*Novel concepts in directed biaryl synthesis, Part XXIX. For Part XXVIII, see ref. 1.

**Author to whom correspondence should be addressed.

SSDI 0020-1693(94)03891-Q

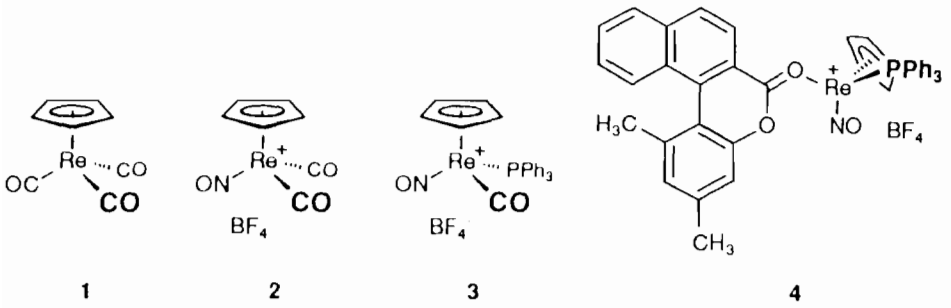

Fig. 1. Structural formulas of the investigated rhenium complexes **1**–**4**.

μm, with a step size of 5 μm, was used [10]. Data were collected in transmission mode with ion chambers. The first ion chamber, monitoring I_0, with a length of 15 cm was continuously flushed with 100% nitrogen. The second and third ion chambers, monitoring I_1 and I_2, respectively, with a length of 30 cm were flushed with a mixture of 74 wt.% argon and 26 wt.% nitrogen. The fill of the ion chambers corresponds to the recommended conditions, i.e. 10% of the incident X-rays will be absorbed in the first ion chamber and 80% in the sample itself [11]. Energy calibration was monitored with a sample of Re_2O_7 in a graphite matrix. Four single scans for each sample in saturated solution were added after they has been examined for a satisfying signal-to-noise ratio, edge energy and absence of anomalies. The rhenium complexes **1–3** are quite stable compounds and they were expected to remain intact during the EXAFS measurement. In contrast, the more labile lactone complex **4** was investigated by NMR spectroscopy before and after the absorption experiment, not only to check homogeneity, but also to exclude a chemical reaction and to make out possible radiation damages. Fortunately, no changes in signal intensity and peak location were observed after the EXAFS measurements, indicating that even the more sensitive complex **4** remained intact throughout the experiments.

3. Data analysis

Data were analyzed with a program package, specially developed for the requirements of liquid and amorphous samples, which is described in detail elsewhere [12] and therefore only a brief summary will be presented here.

The total absorption coefficient $\mu(E)$ is calculated according to

$$\mu(E)d = \ln(I_0/I_1) \tag{1}$$

where E is the energy of the incident X-rays, d is the sample thickness, I_0 and I_1 are the intensities of the incident and the transmitted beam, respectively. The energy threshold E_0 was determined via differentiating the data with respect to E and assigning the first maximum to E_0. The pre-edge absorption coefficient in the range from 10 231.0 to 10 506.0 eV for all investigated compounds was fitted with a Victoreen-type polynomial

$$\mu_v(E) = aE^{-3} + bE^{-4} \tag{2}$$

where a and b are fit parameters. The pre-edge fit is extrapolated beyond the edge and subtracted from the total absorption coefficient to give the edge- and Victoreen-corrected absorption coefficient $\mu_{e,v}(E)$. The interference function above the edge is defined as

$$\chi(E) = [\mu_{e,v}(E) - \mu_0(E)]/\mu_0(E) \tag{3}$$

where the background absorption $\mu_0(E)$ is approximated by a modified smoothing spline function. In order to relate the modulation of the absorption rate in EXAFS $\chi(E)$ to structural parameters, $\chi(E)$ must be expressed in terms of the photoelectron wave vector k.

$$k = \sqrt{(2m/\hbar^2)(E - E_0)} \tag{4}$$

The background removal of spectra of liquid compounds in general and of L_{III}-edge spectra especially is a very sophisticated procedure. Up to about 75 eV above the edge the shape of the Re L_{III}-edge demands a very flexible smoothing spline because of the well pronounced white line. On the other hand, a high flexibility in the range up to about 300 eV above the edge increases the risk of removing or reducing part of the few EXAFS oscillations, which are generally not well pronounced in liquid samples owing to the high static disorder. Additionally, the choice of the first nodal point plays an important role for the shape of the smoothing spline function. An automatic choice of this point, however, is included in most of the existing program packages. Owing to the shape of L_{III}-edge spectra of atoms with free d-orbitals this method can be misleading. We assume to have successfully solved this problem by applying a modified smoothing spline function based on the IMSL subroutine ICSSCU [13, 14], where the possibility of choosing the starting point within a selected range is provided. In this way, the

influence of not only the shape of the edge but also of spurious elements such as over- or undershoots on the shape of $\mu_0(E)$ can be minimized. Fourier transform of k^3-weighted $\chi(k)$ over a finite range between k_{min} and k_{max} yields the modified distribution function in r space where the contributions of one or more backscatterers to the EXAFS function can be isolated by Fourier filtering.

$$F(r) = 1/\sqrt{2\pi} \int_{k_{min}}^{k_{max}} W(k)k^n\chi(k) \exp(i2kr)dk \quad (5)$$

The application of five different window functions, i.e. Square, Welch, Parzen, Hanning and Square/Hanning, which are represented by $W(k)$, helps to detect artificial peaks and sidelobe effects and therefore to select the appropriate r range for the subsequent Fourier filtering. The curve fitting procedure was either performed with amplitude and phase functions from McKale *et al.* [15] or those calculated with the program FEFF (V3.1) [16, 17] implemented in our own program package [12] or, if indicated, the amplitude and phase functions included in EXCURV90. When using the amplitude and phase functions from McKale the amplitude reducing factor S_0^2 was set to 1.0 and the electron mean free path $\lambda(k)$ was approximated by the universal function for inorganic compounds of Teo [8]. Since the program FEFF (V3.1) explicitly calculates these terms, there is no need to set or approximate them. Using EXCURV90 the mean free path of the scattered electron was calculated from the imaginary part of the potential (VPI was set to -4.00) and the amplitude reduction factor AFAC was fixed at 0.8.

Before we discuss the results, some general remarks about the curve fitting must be made. In each case we tried to fit the Fourier filtered range with a minimum set of parameters, i.e. the parameters describing a single shell. If we failed to achieve a good agreement between theoretically calculated function and the Fourier filtered range, step by step an additional backscatterer was added and individually checked for its significance.

When performing single scattering calculations both the coordination number N as well as the Debye–Waller factor σ of the different shells were refined. In order to minimize the strong correlations between these parameters, they were never fitted simultaneously. Nevertheless, we can assume the obtained results for the Debye–Waller factors to contain significant errors. The degree of error for the Debye–Waller term is considerably reduced in the multiple scattering calculations, because the coordination numbers were taken from the structure models and were not allow to vary.

In the Tables for the structural parameters of the four different rhenium complexes standard errors for the absorber–backscatterer distances are given. These errors were derived from the statistical correlations between the parameters in the curve fitting procedure. This is the reason why in some cases there are unexpectedly low values of the order of ± 0.001 Å. A value of such magnitude means that only a distance value in the given small interval produces a best fit result of a comparable quality. The absolute errors of the distances are typically about 0.02 Å or less and for compounds in solution not exactly to determine.

4. Results

The relevant parameters of the data analysis, i.e., the applied weighting scheme, the ranges for Fourier transformation and Fourier filtering, of the investigated compounds **1–4**, are shown in Table 1.

4.1. $CpRe(CO)_3$ in acetone

The results – i.e. the absorber–backscatterer distance r (Å), the corresponding coordination number N, the Debye–Waller factor σ (Å) and the shift of the threshold energy ΔE_0 (eV), obtained with the amplitude and phase functions of McKale *et al.* [15] together with the corresponding standard errors for the distances – are shown in Table 2. The values in parentheses are the corresponding mean distances in the $CpRe(CO)_3$ crystal [18].

When we compared the experimental functions with the theoretically calculated ones, at first sight, the results seemed to be quite satisfying. This first impression was confirmed by the values of the structural parameters for the C(CO) and the C(Cp) backscatterers, as they show only marginal differences compared with the crystal structure data [18]. At second sight, however, there is some conspiciousness about the structural parameters for the O(CO) backscatterer. Firstly, the distance appears about 0.07 Å longer than in the crystal, a fact that is clearly beyond the experimental margin or error. Secondly, the value for the coordination number is about twice as high. Thirdly, the value of the exponential reducing factor σ is definitely too low for a third shell backscatterer. And finally, there are noticeable deviations of the theoretically calculated function from the experimental one in the low k region. Therefore, we tried to describe the experimental $k^3\chi(k)$ function for $CpRe(CO)_3$ with the theoretical functions calculated by the program FEFF [16, 17] in order to rule out possible amplitude and phase inherent effects and to achieve a better agreement in the low k region (FEFF provides the possibility of explicitly calculating the amplitude reducing factor S_0^2 and the electron mean free path $\lambda(k)$, which both have a selective influence on the low k region). These results are given in

TABLE 1. The applied weighting scheme of the EXAFS functions, the ranges for Fourier transformation and Fourier filtering for the compounds **1–4**

	1	**2**	**3**	**4**
Weighting of the EXAFS functions	3	3	3	3
k range for Fourier transformation ($Å^{-1}$)	2.90–16.48	2.93–15.85	2.93–12.72	2.98–9.92
r range for Fourier filtering (Å)	1.35–3.06	1.30–3.20	0.98–2.88	0.68–2.88

TABLE 2. Structural parameters and the corresponding standard errors – absorbers–backscatterer distance r (Å), coordination number N, Debye–Waller factor σ (Å) and the shift of the threshold energy ΔE_0 (eV); obtained by considering single scattering only with the amplitude and phase functions of McKale *et al.* [15], FEFF [16, 17] and EXCURV90 (ss) [19], those obtained by considering multiple scattering effects up to third order, indicated by EXCURV90 (ms, 3) and those obtained with a full multiple scattering calculation indicated by EXCURV90 (ms, f) [20]. Mean crystal structure values [18] are given in parentheses. In the multiple scattering calculations the coordination numbers were taken from the structure model and were not allowed to vary

Backscatterer	r (Å)	N	σ (Å)	ΔE_0 (eV)
McKale				
C(CO)	1.915 ± 0.024 (1.895)	2.06 (3.0)	0.0489	6.38
C(Cp)	2.283 ± 0.030 (2.285)	5.20 (5.0)	0.0829	3.55
O(CO)	3.136 ± 0.013 (3.055)	5.88 (3.0)	0.0494	−9.94
FEFF				
C(CO)	1.939 ± 0.024 (1.895)	2.71 (3.0)	0.0513	4.73
C(Cp)	2.307 ± 0.030 (2.285)	5.54 (5.0)	0.0712	2.65
O(CO)	3.127 ± 0.013 (3.055)	6.59 (3.0)	0.0419	−13.48
EXCURV90 (ss)				
C(CO)	1.891 ± 0.024 (1.895)	2.00 (3.0)	0.0345	
C(Cp)	2.251 ± 0.030 (2.285)	6.41 (5.0)	0.0696	16.01
O(CO)	3.112 ± 0.013 (3.055)	9.70 (3.0)	0.0569	
EXCURV90 (ms, 3)				
C(CO)	1.917 ± 0.001 (1.895)	3.0 (3.0)	0.0501	
C(Cp)	2.290 ± 0.002 (2.285)	5.0 (5.0)	0.0630	20.46
O(CO)	3.056 ± 0.003 (3.055)	3.0 (3.0)	0.0589	
EXCURV90 (ms, f)				
C(CO)	1.919 ± 0.001 (1.895)	3.0 (3.0)	0.0499	
C(Cp)	2.294 ± 0.002 (2.285)	5.0 (5.0)	0.0631	19.48
O(CO)	3.061 ± 0.003 (3.055)	3.0 (3.0)	0.0589	

Table 2. With the FEFF amplitude and phase functions the C(CO) and C(Cp) distances are marginally shifted to higher r values. But, the O(CO) distance (although shifted to a lower r value) and the corresponding coordination number are not realistic. The results obtained with the amplitude and phase functions included in EXCURV90 [19], which are shown in Table 2, show the same conspicious features, e.g. the coordination number for the O(CO) backscatterer appears more than three times as high as it should be. And, the average C–O distance of 1.210 Å (deduced from all these calculations) is too high for coordinated carbonyl groups, which usually show C–O distances between 1.12 and 1.17 Å (see for example refs. 2, 18 and 21).

From all these calculations it can be concluded that different amplitude and phase functions yield the same results within the experimental margin of error. The successful description of the first and second shell may preliminary be interpreted as a proof for the reliability of all the used theoretical functions. Nevertheless, the description of the third shell failed in any case. Chemical effects in solution, however, only concerning the O(CO) parameters are quite improbable. The amplitude enhancement of the third shell, which is artificially taken into account by an increase of the coordination number and a decrease of the Debye–Waller factor must be a method inherent effect. Only multiple scattering can be considering for that effect which is rather probable owing to the linear arrangement of the backscattering atoms C and O in the Re–C–O chain [8, 9]. At this point it must be noted that such strong multiple scattering effects in long and nearly collinear paths were already observed many years ago for corresponding compounds in the solid state, e.g. in $Na_2Fe(CO)_4$ [8].

In order to extract the intrinsic structural parameters we performed multiple scattering calculations with the program EXCURV90 [20]. Step by step higher order scattering paths in addition to the single scattering path Re→O→Re were taken into account. First, the double scattering loops Re→C→O→Re and Re→O→C→Re (each containing one forward scattering event) and subsequently the triple scattering loop Re→C→O→C→Re (containing two forward scattering events). As it can be deduced from Fig. 2 – the contributions of single, double and triple scattering in the linear Re–C–O chain to the EXAFS function and its Fourier transform are shown – there is considerable improvement in the description of the experimental $k^3\chi(k)$ when triple scattering paths are included. The structural parameters obtained by a least-squares refinement procedure including triple scattering paths are shown in Table 2. From the obtained Re–C(CO) and Re–O(CO) distance an average C–O distance of 1.141 Å could be deduced. Because all of the mentioned multiple scattering paths correspond to the same absorber–backscatterer distance as the single scattering Re→O→Re path they all contribute to the same peak in the Fourier transform and cause the so-called focussing or amplitude enhancing effect. Another question is to which extent there are contributions from scattering paths in addition to those in the linear Re–C–O chain. We therefore performed a full multiple scattering calculation including paths in the Cp ring and those combining the Cp ring with the CO groups. These results, shown in Table 2, point out clearly that the mentioned paths combining all fragments in the molecule play only a secondary role. The improvement in the fit index and the change of the values for the structural parameters in comparison to those obtained by including triple scattering paths are marginal. Considering the angles in a scattering loop involving e.g. a C atom of the Cp ring and one of the CO group or

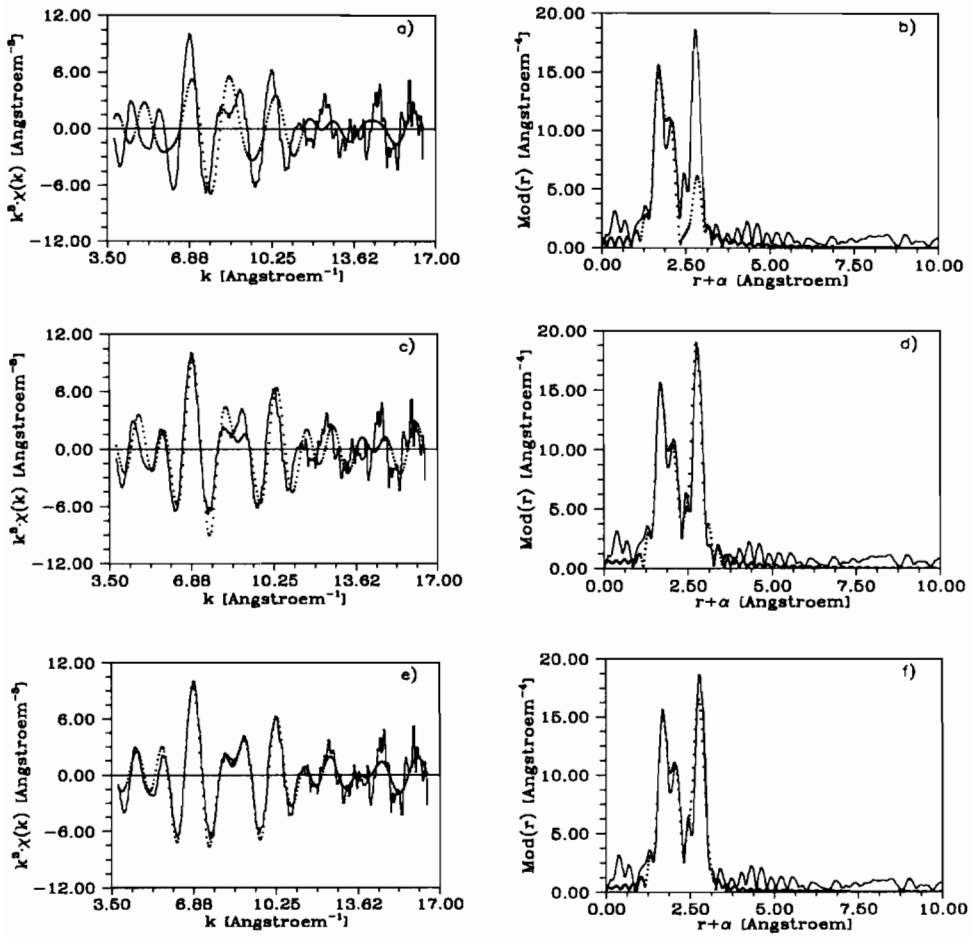

Fig. 2. Experimental $k^3\chi(k)$ function (solid lines in (a), (c) and (e)) and the theoretical function calculated by considering single scattering only (dotted line in (a)), by including double scattering paths (dotted line in (c)) and by including triple scattering paths (dotted line in (e)) within the Re–C–O chain as well as the Fourier transform of the experimental function (solid line in (b), (d) and (f)) and the Fourier transforms corresponding to the different theoretical functions (dotted lines in (b), (d) and (f)) for compound **1**.

two C atoms in the Cp ring, the negligible improvement might be expected. It is well known that the amplitude and phase modification is very much dependent on the angle between the intervening atom and the next nearest neighbor. The greatest effect possible is for angles of 180°, i.e. a linear arrangement, and drops off very rapidly for angles smaller than about 150° [8]. Therefore, the restriction to the mentioned scattering paths in the Re–C–O chain for the description of the experimental $k^3\chi(k)$ function is well justified**.

It is now quite obvious that the common description of EXAFS data with the single-electron single-scattering curved-wave theory yields only unsatisfactory results independent of the used amplitude and phase functions, when strong multiple scattering effects contribute to the EXAFS function. In particular the values for the third shell (Re–O(CO)) are affected. The EXAFS phases are artificially corrected by distance shifts of about 0.07 Å. The amplitude enhancement is shown in a decrease of the exponential damping factor σ and an increase of the coordination number N up to values more than three times as high as it is in reality. The applied multiple scattering formalism included in EXCURV90, however, is able to describe *solution* EXAFS data with a high fraction of forward scattering contributions. The structural parameters for $CpRe(CO)_3$ in acetone solution obtained by considering multiple scattering effects seem to reflect the intrinsic ones. The well defined experimental function and its Fourier transform can be described with realistic parameters without any artificial corrections.

4.2. *[CpRe(CO)$_2$(NO)]BF$_4$ in acetone*

The next link in the synthetic sequence up to the racemic $[CpRe^*(NO)(PPh_3)L]BF_4$ can be deduced from the discussed system by exchange of a CO for an NO ligand. Because the Re–N–O atoms are nearly linearly arranged we expected similar difficulties for the description of the O(CO) and O(NO) parameters using McKale amplitude and phase functions. And indeed, the theoretical description of the experimental function in the low k region was hard to achieve and the resulting values for the coordination numbers of the Debye–Waller factors for the mentioned backscatterers show deviations from the confident values of the same scale as in $CpRe(CO)_3$ (see Table 3). Although the parameters in Table 3 were obtained with the single scattering formalism, they show the tendency to a lower coordination number for the carbonyl oxygen backscatterers of $[CpRe(CO)_2(NO)]BF_4$ compared to $CpRe(CO)_3$.

TABLE 3. Structural parameters and the corresponding standard errors for compound **2**, obtained with the amplitude and phase functions of McKale *et al.* [15] (single scattering) and those obtained by including multiple scattering effects up to third order indicated by EXCURV90 (ms, 3) [20]. In the multiple scattering calculations the coordination numbers were taken from the structure model and were not allowed to vary

Backscatterer	r (Å)	N	σ (Å)	ΔE_0 (eV)
McKale				
N(NO)[a]	1.766 ± 0.027	1.41	0.0890	−0.77
C(CO)	2.006 ± 0.025	1.63	0.0975	8.56
C(Cp)	2.276 ± 0.031	4.90	0.0617	6.01
O(NO)	3.013 ± 0.016	2.47	0.0253	−10.50
O(CO)	3.158 ± 0.014	3.90	0.0338	−10.04
EXCURV90 (ms, 3)				
N(NO)	1.817 ± 0.003	1.0	0.0463	
C(CO)	1.990 ± 0.002	2.0	0.0573	
C(Cp)	2.284 ± 0.004	5.0	0.0606	13.38
O(NO)	2.958 ± 0.007	1.0	0.0335	
O(CO)	3.056 ± 0.006	3.0	0.0551	

[a]Similar organometallic compounds show Re–N(NO) distances between 1.74 and 1.80 Å and Re–O(NO) distances of about 2.97 Å [2, 21–23].

In order to extract the intrinsic parameters we performed multiple scattering calculation with the program EXCURV90, too. The structural parameters obtained by including triple scattering paths within the Re–C–O and the Re–N–O chains are shown in Table 3. As it can be seen in Fig. 3 there is considerable improvement when step by step higher order scattering paths up to triple scattering loops are included. As no further improvement could be achieved with a full multiple scattering calculation for compound **1**, we feel justified in restricting our calculation for compound **2** to the Re–C–O and the Re–N–O chain. Comparing the values in Table 3 it is obvious that not only the parameters of the oxygen backscatterers are influenced by multiple scattering, but also the distance value for the N(NO) backscatterer. Due to the correlation of all the parameters in the EXAFS formula, this could more or less be expected†.

4.3. *[CpRe(CO)(NO)(PPh$_3$)]BF$_4$ in acetone*

In compound **3** a further carbonyl group is exchanged for a PPh_3 ligand and the contribution of multiple scattering paths is expected to be less pronounced than in compounds **1** and **2**. In the curve-fitting procedure, however, we had the same difficulties with the amplitude-affecting parameters N and σ for the carbonyl and nitrosyl oxygen atoms and the description of the low k region was also hard to achieve (see Table 4).

**EXCURV90 additionally provides the possibility of refining the angle for a selected scattering loop. The most significant agreement was obtained for an angle of 180° in the Re–C–O fragment.

†An angle refinement provided the most significant agreement for 180° in the Re–N–O fragment.

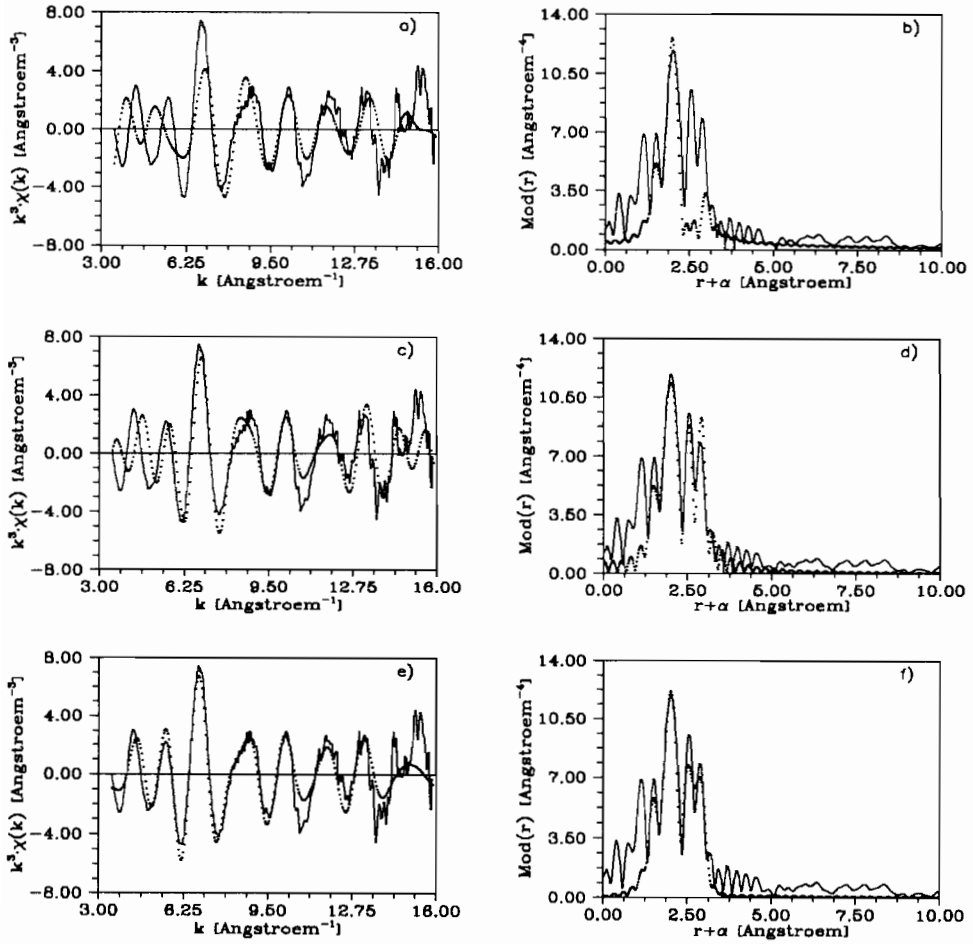

Fig. 3. Experimental $k^3\chi(k)$ function (solid lines in (a), (c) and (e)) and the theoretical function calculated by considering single scattering only (dotted line in (a)), by including double scattering paths (dotted line in (c)) and by including triple scattering paths (dotted line in (e)) within the Re–C–O and the Re–N–O chain as well as the Fourier transform of the experimental function (solid line in (b), (d) and (f)) and the Fourier transforms corresponding to the different theoretical functions (dotted lines in (b), (d) and (f)) for compound **2**.

The multiple scattering calculation revealed the parameters shown in Table 4. The comparison of the values in Table 4 shows that the correlation of the EXAFS parameters is more pronounced for compound **3** for reasons of complexity of the molecule. The differences are most striking for the Re–C(CO) distance, where we obtained 2.092 ± 0.031 Å with single scattering in comparison to 1.933 ± 0.003 Å with multiple scattering. The deduced average C–O and N–O distances are 1.066 and 1.294 Å, respectively (single scattering), and 1.111 and 1.144 Å (multiple scattering).

4.4. [CpRe(NO)(PPh₃)L]BF₄ in CH₂Cl₂*

[CpRe*(NO)(PPh_3)L]BF_4, where L denotes the OCH_3 substituted 'axially prostereogenic' lactone ligand (instead of the dimethylated compound **4**), shows some interesting structural features in the crystalline solid state. It occurs as a racemate but with only one of the two possible helimeric diastereomers and its enantiomer [4]. A comparison of the bond length of the endocyclic carbon atom to the exocyclic oxygen in the OCH_3 derivative (1.254 Å) with that of the free OCH_3-lactone (1.205 Å) shows that the carbonyl bond is weakened due to the coordination to the central rhenium atom. Simultaneously, the endocyclic O–C single bond is significantly shorter in the complex (1.316 Å) than in the free lactone (1.371 Å), indicating an increased π-character of the C–O bond caused by an enhanced electron donating ability of the endocyclic oxygen. This shortening of the C–O bond leads to a slight planarization of the heterocyclic pyranone ring in the complexed lactone. Assuming no structural changes in solution, a nucleophilic attack on the coordinated carbonyl group should occur from one side only, since the other side is shielded by the bulky triphenylphosphine ligand.

Because there is only little knowledge about the properties of these Re–lactone complexes in solution in general, we were interested in the structural features

TABLE 4. Structural parameters and the corresponding standard errors for compound **3**, obtained with the amplitude and phase functions of McKale *et al.* [15] (single scattering) and those obtained by including multiple scattering effects up to third order indicated by EXCURV90 (ms, 3) [20]. In the multiple scattering calculations the coordination numbers were taken from the structure model and were not allowed to vary

Backscatterer	r (Å)	N	σ (Å)	ΔE_0 (eV)
McKale				
N(NO)	1.729 ± 0.034	1.22	0.0446	−6.22
C(CO)	2.092 ± 0.031	0.95	0.0978	−1.20
C(Cp)	2.295 ± 0.039	4.65	0.0647	5.47
P(PPh_3)[a]	2.365 ± 0.032	1.14	0.0503	5.69
O(NO)	3.023 ± 0.020	2.61	0.0393	−6.16
O(CO)	3.158 ± 0.017	2.72	0.0585	−8.04
EXCURV90 (ms, 3)				
N(NO)	1.758 ± 0.004	1.00	0.0608	
C(CO)	1.933 ± 0.031	1.00	0.0592	
C(Cp)	2.283 ± 0.039	5.00	0.0613	17.17
P(PPh_3)	2.348 ± 0.032	1.00	0.0551	
O(NO)	2.902 ± 0.020	1.00	0.0571	
O(CO)	3.104 ± 0.017	1.00	0.0567	

[a]Similar organometallic compounds show Re–P(PPh_3) distances between 2.35 and 2.45 Å [2, 21–23].

such as types of backscatterers and bond lengths for complex **4**. The aim of our investigations was to study the EXAFS spectroscopical behavior of the relatively stable lactone complexes of type **4**, which are characterized by crystal structure analysis, and then to investigate the intermediates, which are assumed to be very instable and hitherto not isolable lactolates, in solution. Despite the fact that crystal structure data were available for the OCH_3 substituted lactone complex [4], we chose the CH_3 substituted analogue **4**. Compound **4** was expected to show a more simple physical behavior mainly due to the presence of fewer atoms contributing to the background absorption.

We could not perform the measurement for compound **4** in acetone solution, because a coordination of this solvent via the carbonyl function may not be excluded. Therefore we had to chose a non-coordinating solvent like CH_2Cl_2 in order to guarantee the chemical intactness of the Re–lactone complex. And, the investigated complex shows a sufficient solubility in CH_2Cl_2. From an EXAFS spectroscopical point of view, however, the background absorption due to the chlorine atoms and the atoms with large distances from the absorbing atom, i.e. the carbon atoms of the lactone and the triphenylphosphine group, is enhanced. The consequences are a bad signal-to-noise ratio, only weakly pronounced oscillations, a very small usable k range and therefore a low resolution in r space. The results of the very carefully performed curve-fitting procedure with amplitude and phase functions of McKale *et al.* [15] are shown in Table 5.

We identified about one N backscatterer at 1.700 Å, which can be unambiguously assigned to the nitrosyl-N (1.75 Å in the crystal), the carbon atoms of the Cp ring at 2.276 ± 0.065 Å (2.19–2.24 Å in the crystal), the phosphorous atom of the triphenylphosphine ligand at 2.380 ± 0.041 Å (2.39 Å in the crystal) and an oxygen backscatterer at 2.051 ± 0.051 Å. Comparing this value with the crystal structure data for the complex with the OCH_3 derivative, where the distance of the exocyclic oxygen to the central rhenium atom is 2.11 Å, an assignment to the coordinating exocyclic oxygen is justified. The difference of 0.06 Å may be a consequence of either chemical effects or, which is more likely, a systematic error caused by the high noise level of the experimental spectrum. The second O backscatterer at 2.954 ± 0.026 Å was assigned to the oxygen atom of the nitrosyl group for the following reasons. Firstly, it definitely cannot be the contribution of the endocyclic oxygen, since the $Re–O_{endo}$ distance in the complex with the OCH_3 derivative is 3.27 Å [4]. The difference of 0.32 Å is clearly beyond the experimental margin of error. Secondly, the very high coordination number of 3.10 and the low Debye–Waller factor hint at a backscattering path markedly influenced by multiple scattering effects.

The structural parameters obtained by including multiple scattering effects in the Re–N–O chain up to third order are shown in Table 5. Multiple scattering effects seem to have an influence not only on the distance and coordination number of the O(NO) backscatterer. A comparison of the values in Table 5 points out deviations even for the distance of the N(NO) and the

TABLE 5. Structural parameters and the corresponding standard errors for compound **4** [4], obtained with the amplitude and phase functions of McKale *et al.* [15] (single scattering) and those obtained by including multiple scattering effects up to third order indicated by EXCURV90 (ms, 3) [20]. In the multiple scattering calculations the coordination numbers were taken from the structure model and were not allowed to vary

Backscatterer	r (Å)	N	σ (Å)	ΔE_0 (eV)
McKale				
N(NO)	1.700 ± 0.043	1.30	0.0213	−11.53
O	2.051 ± 0.051	1.93	0.0398	4.16
C(Cp)	2.276 ± 0.065	4.61	0.0791	3.30
P(PPh_3)	2.380 ± 0.041	1.38	0.0315	8.53
O	2.954 ± 0.026	3.10	0.0202	−10.64
EXCURV90 (ms, 3)				
N(NO)	1.763 ± 0.005	1.00	0.0608	
O	2.108 ± 0.006	1.00	0.0531	
C(Cp)	2.284 ± 0.008	5.00	0.0791	12.38
P(PPh_3)	2.357 ± 0.005	1.00	0.0563	
O	2.907 ± 0.010	1.00	0.0503	

$P(PPh_3)$ backscatterer as well as for the coordinated lactone. On the one hand, this makes an assignment of the identified O backscatterer at 2.108 ± 0.006 Å to the coordinated lactone much clearer. Furthermore, the Re–N(NO) of 1.763 ± 0.005 Å compared to 1.75 Å in the crystal seems to be more realistic. On the other hand, the obtained Re–O(NO) distance of 2.907 ± 0.010 Å leads to an average N–O distance of 1.144 Å, which is – compared with the crystal structure value of 1.211 Å [4] – too short. The average N–O distance of 1.254 Å deduced from single scattering calculations, however, is too long but within the experimental margin of error.

Basing upon the identified types of backscatterers and the obtained distance values we conclude that the structure of $[CpRe^*(NO)(PPh_3)L]BF_4$ is preserved in CH_2Cl_2 solution. No further significant contributions to the EXAFS function of this compound could be detected. The problems in describing the EXAFS function of compound **4** make it clear that the results have only a preliminary character. Nevertheless, they show that the investigation of a series of related compounds with an increasing degree of complexity helps to make out the individual characteristic features of the EXAFS functions. And, it facilitates the interpretation of subsequent EXAFS measurements of compound **4** or its analogues. A potential approach to shed additional light on the structure of $[CpRe(NO)(PPh_3)L]BF_4$ in solution may be to increase the solubility of this compound in a less delicate solvent, i.e. a solvent which does not contain halogens or any other highly absorbing atoms. Nearly all common non-chlorine containing polar solvents, e.g. acetone or alcohols, show a more or less pronounced coordinating ability. Therefore, the solubility in a non-polar solvent should be increased by, e.g. a substitution of the coordinated lactone with long-chain alkyl residues. It is not known how far the charged nature of the complex decreases the solubility in non-polar solvents and this problem would of course remain.

5. Discussion

We have presented the results of an EXAFS study of a chiral rhenium complex with an 'axially prostereogenic' biaryl lactone as ligand and its precursors in CH_2Cl_2 and acetone solution, respectively. The results of the data analysis for $CpRe(CO)_3$, the first link in the synthetic sequence up to the chiral $[CpRe^*(NO)(PPh_3)L]BF_4$, obtained with the commonly used single-electron single-scattering curved-wave theory are reliable for those backscattering paths which are only marginally influenced by multiple scattering effects, i.e. the C(CO) and the C(Cp) backscatterers. The structural parameters for the O(CO) backscatterers, however, could only be described with an often used and reliable multiple scattering formalism (see for example refs. 19, 20 and 24).

A comparison of the parameters obtained with the curved-wave theory with those obtained by including multiple scattering allows the deviations caused by forward scattering effects to be estimated reasonably accurately. The Re–C(CO) and Re–N(NO) distances obtained with the single scattering theory are (on an average) shifted 0.07 ± 0.035 Å to higher r values and the coordination numbers appear 2.4 ± 0.5 or 2.7 ± 0.03 times, respectively, too high. Such a comparative procedure provides the possibility to estimate structural parameters for related compounds for which a treatment with the multiple scattering formalism is not applicable for reasons of complexity of the molecule or due to the data quality. The correlation of the structural parameters within one absorber–backscatterer pair and between the different coordination shells, however, makes it difficult to transfer determined calibration factors. An EXAFS spectroscopical investigation of a series of compounds, like complexes **1–3**, with known structures and an increasing degree of complexity is a great help for interpreting the EXAFS function and the obtained structural parameters for a related compound like **4** for which the structure in solution is unknown. An impressive example is the assignment of the Re–O distance of 2.954 ± 0.026 Å to the nitrosyl oxygen due to the artificially high coordination number and the very low Debye–Waller factor, which are unambiguous indications of a multiple scattering effect. This assignment was confirmed by the subsequent, but nevertheless preliminary, multiple scattering calculation with EXCURV90.

As mentioned above, a potential approach to overcome the not always sufficient solubility of the lactone complexes of type **4** in non-polar solvents and thus to get good-quality EXAFS spectra, will be to increase the solubility by appropriate substitution. The first investigation of a chiral rhenium biaryl lactone complex – based upon multiple scattering calculations of the precursors – is a first and very promising step on our way to establish a reliable procedure to get structural information in solution, starting with a class of substances which is well known from crystal structure analysis and then to go over to mechanistically relevant intermediates of the stereoselective ring-opening process, e.g. rhenium lactolates, which, for reasons of instability, will possibly be characterized with respect to the metal environment by EXAFS only.

Acknowledgements

We thank the SFB 347 ('Selektive Reaktionen Metallaktivierter Moleküle') for generous financial support

as well as the Hamburger Synchrotronstrahlungslabor (HASYLAB) at DESY, Hamburg, for the provision of synchrotron radiation. The authors T.S.E. and H.B. thank the Dr Leni-Schöninger Stiftung and the Stipendienfonds des Verbandes der Chemischen Industrie for generous financial support.

References

1 G. Bringmann and T. Hartung, *Tetrahedron, 49* (1993) 7891.
2 D.M. Dalton, J.M. Fernándes, K. Emerson, R.D. Larsen, A.M. Arif and J.A.Gladysz, *J. Am. Chem. Soc., 112* (1990) 9198.
3 W. Tam, G.-Y. Lin, W.-K. Wong, W.A. Kiel, V.K. Wong and J.A. Gladysz, *J. Am. Chem. Soc., 104* (1982) 141.
4 G. Bringmann, O. Schupp, K. Peters, L. Walz and H.G. von Schnering, *J. Organomet. Chem., 438* (1992) 117.
5 G. Bringmann, R. Walter and R. Weirich, *Angew. Chem., Int. Ed. Engl., 29* (1990) 977.
6 G. Bringmann, H. Busse, S. Güssregen, B. Schöner, O. Schupp and R. Walter, in H. Werner, A.G. Griesbeck, W. Adam, G. Bringmann and W. Kiefer (eds.), *Selective Reactions of Metal-Activated Molecules,* Vieweg, Braunschweig, Germany, 1992, p. 183.
7 G. Bringmann, O. Schupp and L. Göbel, *GIT Fachz. Lab., 3* (1993) 189.
8 B.K. Teo, *EXAFS: Basic Principles and Data Analysis,* Springer, Berlin, 1986.
9 D.C. Koningsberger and R. Prins, *X-Ray-Absorption: Principles, Applications, Techniques of EXAFS, SEXAFS and XANES,* Wiley, New York, 1988.
10 T.S. Ertel and H. Bertagnolli, *Nucl. Instrum. Methods Phys. Res., Sect. B, 73* (1993) 199.
11 P.A. Lee, P.H. Citrin, P. Eisenberger and B.M. Kincaid, *Rev. Mod. Phys., 53* (1981) 769.
12 T.S. Ertel, H. Bertagnolli, S. Hückmann, U. Kolb and D. Peter, *Appl. Spectrosc., 46* (1992) 690.
13 A. Proctor, J.M. Fay, D.P. Hoffmann and D.M. Herkules, *Appl. Spectrosc., 44* (1990) 1052.
14 *FORTRAN Subroutines for Mathematical Applications,* Version 1, IMSL, Houston, TX, 1987.
15 A.G. McKale, B.W. Veal, A.P. Paulikas, S.K. Chan and G.S. Knapp, *J. Am. Chem. Soc., 110* (1988) 3763.
16 J.J. Rehr, R.C. Albers and J. Mustre de Leon, *Physica B, 158* (1989) 417.
17 J.J. Rehr, J. Mustre de Leon, S.I. Zabinsky and R.C. Albers, *J. Am. Chem. Soc., 113* (1991) 5135.
18 P.J. Fitzpatrick, Y. Le Page and I.S. Butler, *Acta Crystallogr., Sect. B, 37* (1981) 1052.
19 S.J. Gurman, N. Binsted and I. Ross, *J. Phys. C, 19* (1986) 1845.
20 S.J. Gurman, *J. Phys. C, 21* (1988) 3699.
21 I. Saura-Llamas, D.M. Dalton, A.M. Arif and J.A. Gladysz, *Organometallics, 11* (1992) 683.
22 C.M. Garner, N.Q. Méndez, J.J. Kowalczyk, J.M. Fernández, K. Emerson, R.D. Larsen and J.A. Gladysz, *J. Am. Chem. Soc., 112* (1990) 5146.
23 J.H. Merrifield, C.E. Strouse and J.A. Gladysz, *Organometallics, 1* (1982) 1204.
24 N.J. Blackburn, R.W. Strange, L.M. McFadden and S.S. Hasnain, *J. Am. Chem. Soc., 109* (1987) 7162.